Advanced Monitoring and Conservation Strategies for Wall Paintings Impacted by Microbiological Degradation and Clay Minerals at Al-Qurna, Thebes West Bank (Luxor)

Abubakr Moussa * and Amr Osman

Posted Date: 10 May 2024

doi: 10.20944/preprints202405.0634.v1

Keywords: Microorganisms; Clay minerals; Wall paintings; Al-Qurna; Thebes; Luxor; Monitoring; Conservation Strategies

Article

Advanced Monitoring and Conservation Strategies for Wall Paintings Impacted by Microbiological Degradation and Clay Minerals at Al-Qurna, Thebes West Bank (Luxor)

Abubakr Moussa [1,*] and Amr Osman [2]

[1] Department of Conservation, Faculty of Archaeology, Cairo University, 12613 Orman, Giza, Egypt); dr_abubakr@cu.edu.eg
[2] Department of Conservation, Faculty of Archaeology, Sohag University, 82524 Sohag, Egypt); amr.osman@arch.sohag.edu.eg
* Correspondence: dr_abubakr@cu.edu.eg; Tel.: +20-(10)-9666-4411

Abstract: This paper investigates the influence of microorganisms and clay minerals on the deterioration process of ancient Egyptian murals in the Al-Qurna region, situated on the west bank of Thebes (Luxor), Egypt. To achieve this objective, an extensive examination of building materials (including bedrock, building stone, mortars, and plasters) from various tombs within the study area was conducted. The investigation employed a multidisciplinary approach, combining micro-biological analysis with advanced techniques such as X-ray diffraction (XRD), X-ray fluorescence (XRF), scanning electron microscopy with energy dispersive spectroscopy (SEM-EDS) as well as petrographic examination. These methods were employed to identify the composition of the materials and to assess the masonry structure's response to deformation caused by endogenous factors, particularly clay minerals. Additionally, mycological analyses were performed using a swabbing cotton sterile technique, revealing the presence of several species, including *Ascosphera apis*, *Aspergillus tamarii*, *Aspergillus ochraceus*, *Doratomyces sp*, and *Eurotium repens*. Notably, swelling clays—such as smectite, illite, and chlorite—along with mixed layers of illite-smectite and illite-vermiculite were detected in the studied samples. The presence of such deleterious clay minerals and fungi imperils wall painting preservation, causing discoloration, surface alteration, physical decay, and structural instability. Informed conservation strategies must address these threats for sustained integrity.

Keywords: microorganisms; clay minerals; wall paintings; Al-Qurna; Thebes; Luxor; monitoring; conservation strategies

1. Introduction

Situated on the western bank of the Nile in Thebes, Al-Qurna is positioned at coordinates 25.67° N 32.70° E, with an elevation of approximately 88 meter / 288 feet above sea level (ASL). It is roughly 900 km (560 miles) south of Cairo (see Figure 1). Al-Qurna is a historical village, with its residences constructed atop an archaeological site (Figure 2a). The entire region, encompassing Al-Qurna and the Nile valley, was a site of significant land formation and movement in the remote geological past. Over thousands of years, the Mediterranean Sea repeatedly encroached upon and submerged much of present-day Egypt, reaching as far south as Aswan, due to oscillating ocean levels. This resulted in the deposition of three consecutive sedimentary rock layers, namely the Dakhla chalk, Esna shale, and Theban limestone, familiar to geologists. The latter two layers are primarily visible on the west bank of Thebes, with the limestone layer being about 300 m thick from its peak to where it blends into the underlying shale layer, which is approximately 60m thick. The boundary between these distinct sedimentary layers can be observed at various locations in Al-Qurna and even inside some of the tombs. The area's rock formations are fractured by numerous geological faults due to the ancient depletion of groundwater and subsequent earth movement over time (Figure 2b).

Preprints.org (www.preprints.org) | NOT PEER-REVIEWED | Posted: 10 May 2024 doi:10.20944/preprints202405.0634.v1

Figure 1. The location of the study area (Source: https://geology.com/world/egypt-satellite-image.shtml).

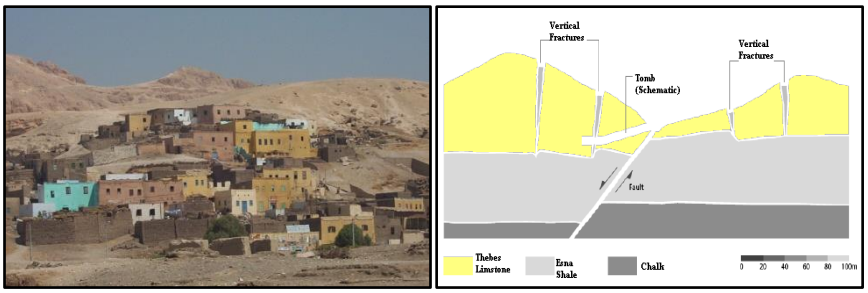

(a) **(b)**

Figure 2. (a): The village of Al-Qurna which is built upon the archaeological site carrying the same name (after Moussa 2007). (b): The fractures and faults affecting the rock-cut tombs at Al-Qurna (after Theban mapping project 2006).

The rock structures of Thebes also display hundreds of open cracks, which are not classified as geological faults since they exhibit no evidence of displacement on either side. These rock joints, as they are known to geologists, are particularly prominent in the lower Valley of the Kings and were frequently utilized by ancient stonecutters when choosing tomb locations and carving the tombs. Initially, the builders selected the soft shale layer for the construction of underground tombs, considering the excavation tools available at that time. However, as shale is prone to slaking, the tombs encountered some stability issues in the roof. Consequently, they likely opted for limestone as the roof material while the sidewalls and floor remained within the shale layer. Nevertheless, the limestone layer directly above the shale formation is highly jointed, leading to roof stability problems for large span excavations once again. As excavation techniques and tools improved and understanding of rock properties deepened over time, the tomb builders began to select the soft limestone layer for the construction of underground tombs. In some cases, the tombs appear to have been designed and constructed in alignment with the geometry of the soft limestone layer. The area's natural topography made it an ideal location for a royal necropolis, while the secluded valleys beyond offered numerous sites for the construction of exquisite rock-cut tombs [1–10].

Among all the hazards facing the Kings' Valley (KV), the most severe (and most preventable) is the flooding caused by heavy rainfall that hits the Valley's watershed. These sudden downpours can generate flash floods in minutes, sweeping tons of debris down the KV slopes and into unprotected tombs. The floodwaters erode the bedrock in which the tombs are carved, ruin their decorated walls, deposit several meters of silt and stone in their chambers, and induce significant and damaging changes in the humidity levels within the tomb chambers [11,12]. The wall paintings found in Al-Qurna, hold immense historical and cultural importance. These ancient artworks provide invaluable insights into Egyptian civilization. Scholars from diverse fields, including Egyptology [2,4,13,14]

 doi:10.20944/preprints202405.0634.v1

architecture, decoration [15–18] and historical research [19], have extensively studied these tombs. Additionally, investigations have explored aspects of damage and their causative factors affecting these antiquities, prompting discussions on restoration strategies and mitigation methods. Despite their significance, the wall paintings in Al-Qurna encounter several conservation challenges, including natural deterioration, climatic influences, and anthropogenic activities such as tourism and vandalism. Ongoing efforts aim to safeguard these invaluable cultural artifacts, ensuring their preservation for future generations.

The process of atmospheric weathering of mined aggregates has the potential to generate clay minerals. The expansion of these clay minerals can exert enough pressure to fracture the building materials [20]. Microscopic fungi, which thrive in environments exposed to the atmosphere, play a significant role in this process. Enhancing the durability of archaeological structures can only be achieved through a comprehensive understanding of the deterioration mechanisms. As evidenced by other inorganic materials such as stones, mortars, plasters, and pigments, it is crucial to focus on the interactions between materials and microorganisms, as well as the processes of microbial degradation [21]. Within this context, this study assumes critical importance as it investigates the impact of key factors contributing to damage affecting wall paintings in several tombs within this region. Specifically, the research examines the effects of deleterious clay minerals and microbiological agents on all mural components—from the stone or clay substrates to the various layers of construction and ultimately the surface and pigments of the wall paintings. By comprehending the nature of these threats and their underlying mechanisms, this study seeks to mitigate risks to the stability and long-term preservation of these artworks. The primary objective of the present research is to evaluate the influence of microorganisms and clay minerals on the degradation process of ancient Egyptian murals at Al-Qurna. This evaluation is conducted through the application of chemical and physical analyses. The insights gained from these analyses could be instrumental in accurately interpreting the progression of damage. Consequently, the findings of this study could potentially be generalized and applied to analogous situations experiencing similar issues.

2. Materials and Methods

In situ, an initial visual examination and photographic documentation of deterioration aspects were conducted. Subsequently, few representative samples -due to restrictions given by authorities - were meticulously extracted from diverse locations in Thebes, employing manual techniques involving chisel and hammer. These samples were subsequently scrutinized using a Nikon SMZ18 stereomicroscope equipped with a Nikon DS-Ri2 microscope camera. Regarding to the biological aspect of the study, Czapeck's medium [22,23] was employed for the isolation and cultivation of microorganisms. For each sample, three duplicate plates were prepared. Following an incubation period of one week at 28 °C, fungal colonies were purified utilizing Martin medium. The purified fungal isolates were then identified using PDA medium, which served as a slant stock culture for fungi, as per the methodology outlined by Barnett et al., 1972 [24], Domsch et al., 1980 [25], Stevens 1981 [23] and Hemraj et al., 2013 [26]. Isolates were identified on the basis of: 1- Gram-stain reaction of smears. 2- Shape: The shapes of fungal cells were microscopically examined at a magnification of 1500x. 3- Motility: this was examined by the hanging drop technique using broth cultures old 18 – 20 hrs. 4- Sporulation: the presence, shape and position of spores'-stained smears were noticed using brilliant green pigmentation. Bio-chemical tests were also carried out by a typical procedure based on Bergey's manual 2008 [27].A thin section with a certain thickness of ca. 30 μm of some samples was prepared by embedding intact piece with low viscosity epoxy resin under vacuum [28]. A set of overlapping photomicrographs was captured under Zeiss Axiolab Opton polarizing microscope connected with Canon Powershot G2 camera jointed to the microscope through an eyepiece adapter [29] for certain samples, then automatically stitched together using Adobe Photoshop CS3 software for image analysis purposes. Approximate constituents' proportions and Grains' sizes have been obtained by point counting and grain length options respectively by JMicrovision V.1.2.7 software [30–33].

 doi:10.20944/preprints202405.0634.v1

The study employed X-ray diffraction (XRD) analysis, utilizing a Philips (PW1840) diffractometer equipped with Ni-filtered Cu-Kα radiation. The samples underwent scanning across 3-63° 2θ intervals at a rate of 1.2° min-1. The XRD data was used to quantitatively estimate the abundance of mineral phases, based on the intensity of specific reflections and external standard mixtures of minerals, in comparison with the JCPDS standards of 1967 [34].

Micro-XRF analyses were conducted using a SPECTRO COPRA "Compact Portable Roentgen Analyzer" diffractometer, with a potential acceleration of 35 kV, lamp stream of 0.9 mA, and an analysis time of 300 seconds. For SEM-EDS analyses, samples were coated using the JEOL JEE-4X High vacuum evacuator with carbon coating (carbon rods). The SEM used was the JEOL JSM-840A, equipped with an EDS analytical attachment from OXFORD instruments ISIS, operating at a working distance (WD) of 20 mm, a current of 1mA, and an accelerating voltage of 20 kV.

In the clay mineralogy study, the grain size of the material was determined and a textural classification was performed on each sample, following the method proposed by Folk (1968) [35]. A 20g fraction of each sample was subjected to a series of chemical treatments (Jackson, 1974) [36]: a 1N sodium acetate-acetic acid buffer solution with pH=5.0 for carbonate removal; 30% H_2O_2 for organic matter and Mn-oxides removal; and a 0.3M sodium citrate and 1M sodium bicarbonate buffer solution with pH=7.3, to which 1g increments (up to 3 g) of sodium dithionite were periodically added to remove free Fe-oxides and Fe-Al-hydroxides.

Particulate fractions smaller than 2 microns were fractionated into three distinct size ranges (2–1 μm, 1–0.25 μm, and <0.25 μm) using an International Equipment Company (IEC) centrifuge. After separation, the sample fractions were air-dried at room temperature. Both random and oriented mounts were then carefully prepared for XRD analysis. Notably, all oriented mounts were reanalyzed after treatment with an ethylene-glycol solution, a process aimed at identifying the expandable mineral phases. Additionally, a subset of these mounts was subjected to a heat treatment at 550°C for two hours to facilitate the detection of chlorite.

These analytical steps contribute to a comprehensive understanding of the mineralogical composition within the studied samples [37]. Semi-quantitative assessments of mineral abundance were derived from the peak areas observed in the oriented mounts, following the methodology outlined by Biscaye (1965) [38].

3. Results

3.1. Initial Visual Examination

Through the field visit and initial visual inspection of a number of wall paintings in the various Theban structures including tombs of Daji (TT 103), Ra'Mosses (TT 046), Userhat (TT 056), Rekhmire (TT 100), Kha' Em Het (TT 057), Amen Em Hab (TT 278) and Amenwahsu (TT 111), a diverse range of damage affecting various components of the wall paintings has been observed. That includes all the elements of the wall paintings, commences with the foundational building materials, extends through the layers of plaster, and culminates to the pigments applied to the surface. The observed damage encompasses separations, collapses, cracks, staining, and fading. Detailed figures illustrating these phenomena are provided in Figure 3.

 doi:10.20944/preprints202405.0634.v1

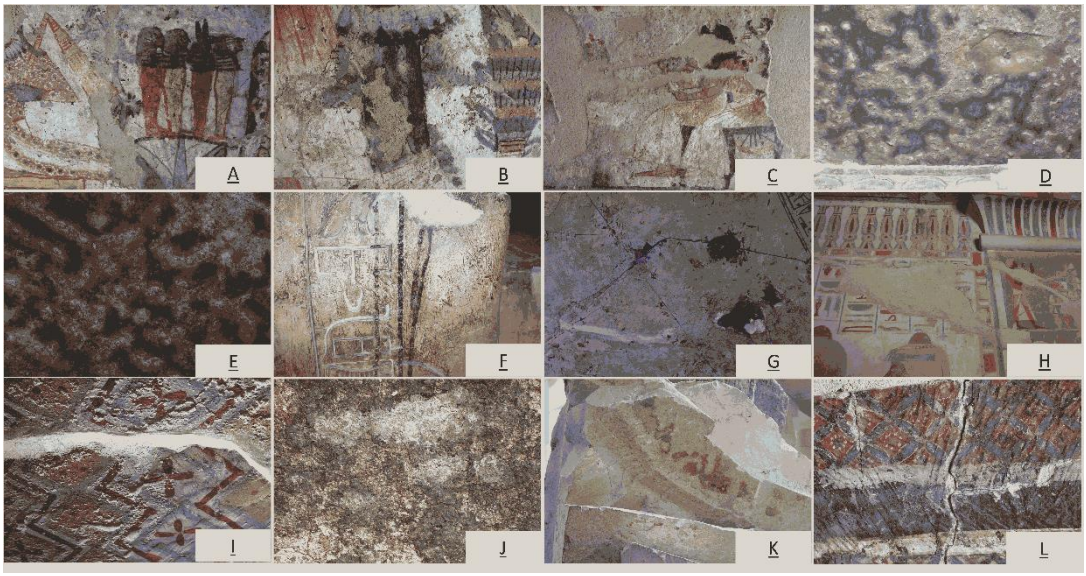

Figure 3. Initial Visual inspection in situ shows various deterioration aspects on wall painting from different tombs at Al-Qurna including peeling in A & B fading in D & E, cracking in K & L, powdering in I, cracking in G & L, discoloration in J and structural instability in C & H and K.

3.2. Microbiological Study

The microbiological examination revealed that the fungal population, particularly *Ascosphaera apis*, is the dominant fungal species, accounting for 25% of the overall fungal isolates extracted from the studied area. This fungal strain shows a significant affinity for pigments in shades of blue, black, and green especially within the tomb of Rekhmire. It was also detected near the sandstone columns in Madinet Habu temple.

Among the identified Aspergillus species, the *Aspergillus tamarii* group (comprising 20% of the isolates) was found to target the white pigment in the tomb of Daji and the sandstone columns in Madinet Habu temple. *Aspergillus ochraceus* (constituting 15% of the isolates) primarily attacked the blue pigment within Userhat tomb and was also identified in samples taken from the tomb's internal air.

In addition, *Doratomyces spp* exclusively affected the blue color within Ra' Mosses tomb. Interestingly, the fungal group *Eurotium chevalieri* was exclusively associated with the black color within Rekhmire tomb. Moreover, both *Aspergillus tamarii* and *Aspergillus ochraceus* were also detected on the blue and black pigments in the tombs of Ra' Mosses and Rekhmire.

Beyond these specific species, other genera isolated included *Eurotium chevalieri*, which was found on white pigment in Daji tomb, as well as on the green and blue pigments within Madinet Habu temple. Lastly, the fungal species *Eurotium repens* was exclusively detected in samples taken from the sandstone blocks of Madinet Habu temple's walls.

The outcomes of the microbiological investigation can be visually represented through the utilization of the following Figure 4 and Table 1.

 doi:10.20944/preprints202405.0634.v1

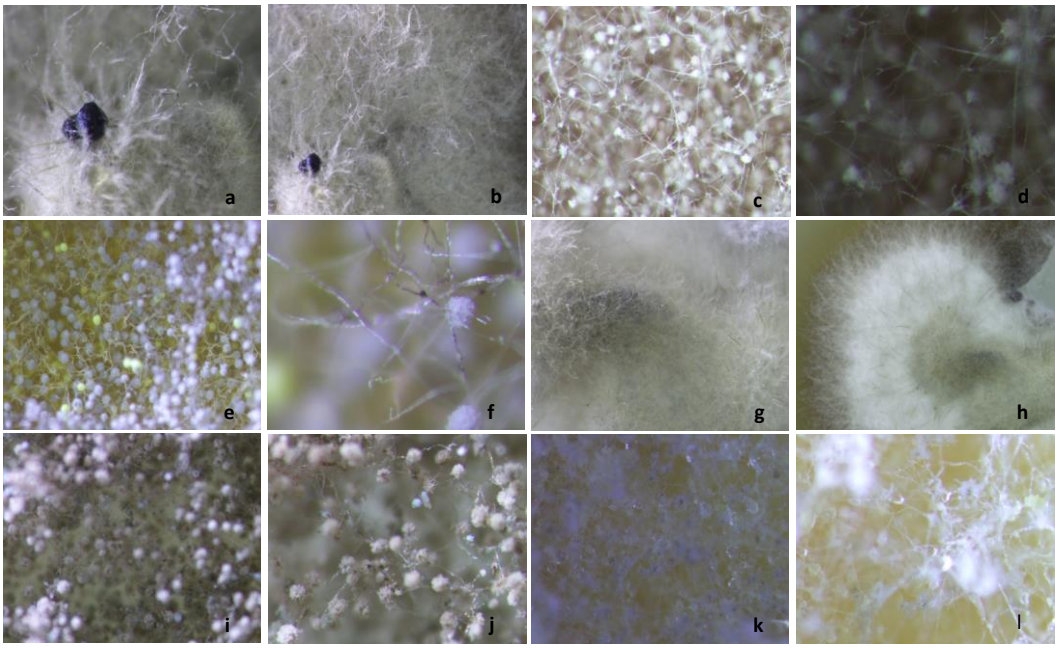

Figure 4. a and b show Ascosphaera apis; c and d show Aspergillus ochraceus; e and f show Aspergillus tamarii; g and h show Doratomyces spp; I and j show Eurotium chevalieri; k and l show Eurotium repens.

Table 1. summerize the qualitative and quantitative outcomes of the microbiological investigation.

Isolated fungal species	No. of isolates	Percentage %
Ascosphaera apis	5	25
Aspergillus tamarii	4	20
Aspergillus occhraceus	3	15
Doratomyces spp	1	5
Eurotium chevalieri	1	5
Aspergillus tamarii + Aspergillus occhraceus	4	20
Eurotium repens	2	10
Total isolates	20	100 %

3.3. XRD & μ-XRF Anlysis and Petrographic Analysis

The results obtained from (XRD) and (μ-XRF) analyses of the samples collected from the bedrock, limestone, cement material, and mortars are presented in Figure 5. The predominant bedrock sample composition 'Esna Shale' indicates that clay minerals (illite-smectite) constitute the major phases (38%), while calcite ($CaCO_3$) (24%), dolomite $CaMg(CO_3)_2$ (22%), quartz (SiO_2) (10%), and halite (Na.Cl) (6%) were also identified. The μ-XRF analysis of the rock samples from the tomb-cutting areas confirms their composition as primarily 'Esna Shale.' The local rock exhibits metamorphic features, having transformed from dolomite to clayey stone ('marl') with the presence of quartz and a significant proportion of precipitated NaCl between the clay nodules [Figure 5e,i and Table 2]. XRD analyses conducted on the hard limestone within the study area unequivocally confirm its composition as pure calcite (100%) [Figure 5f]. In contrast, an additional limestone sample (soft limestone) exhibits clacite, dolomite and anhydrite by XRD as depicted in Figure 5g. This soft limestone sample is characterized by the following mineral proportions: Dolomite ($CaMg(CO_3)_2$): 44%, Anhydrite ($CaSO_4$): 29%, Calcite ($CaCO_3$): 27%. An investigation was carried out on a specimen obtained from the cement substance situated among the limestone strata structures in the vicinity [Figure 5h]. The findings revealed the composition to be 96% calcite ($CaCO_3$), 2% quartz(SiO_2), and 2% of halite (Na.Cl). With the μ-XRF Figure 5k, Fe found as one of the detected elements, which may

 doi:10.20944/preprints202405.0634.v1

refer to atmospheric pollution than pyrite. Regarding the clay mortars, it was demonstrated that they contain a blend of quartz and calcite. These substances were incorporated into the mortar as filler materials. Additionally, Anhydrite was detected in the sample through XRD analysis. As for the two Hiba mortars they revealed similarity of chemical composition of $CaCO_3$, Fe_2O_3, $CaSO_4$, SiO_2 and clays as detected by μ-XRF. The identical findings were confirmed through the use of SEM-EDS and XRD analysis in one specimen. However, a slight variation in the chemical composition was observed in another specimen, which was manifested in the presence of Cu and trace amounts of the plagioclase "albite".

Table 2. μ-XRF results of Mineral oxides found in the Esna shale.

Component	% m/m	± std.
SiO_2	17.4	0.7
K2O	0.77	0.02
CaO	9.6	0.8
TiO_2	0.15	0.02
MnO	430 ppm	20 ppm
Fe_2O_3	1.83	0.06

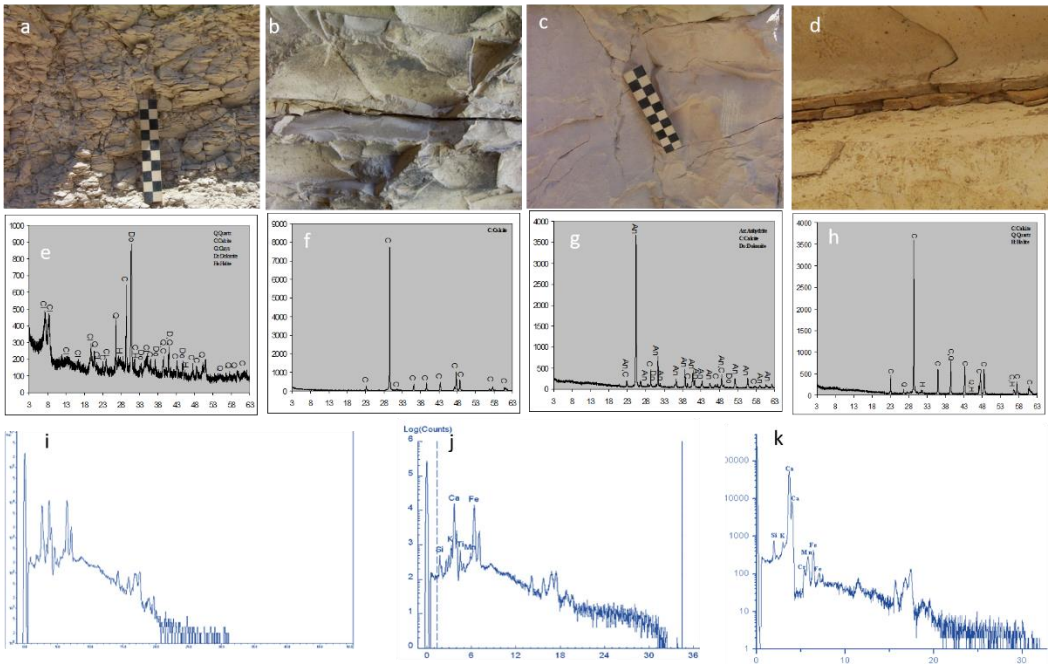

Figure 5. a) Esna shale; b) hard limestone; c) soft limestone; d) cement material; e, f, g and h) XRD patterns of Esna shale, hard limestone, soft limestone, and cement material respectively; i, j and k) μ-XRF patterns of Esna shale, limestone, and cement material respectively.

 doi:10.20944/preprints202405.0634.v1

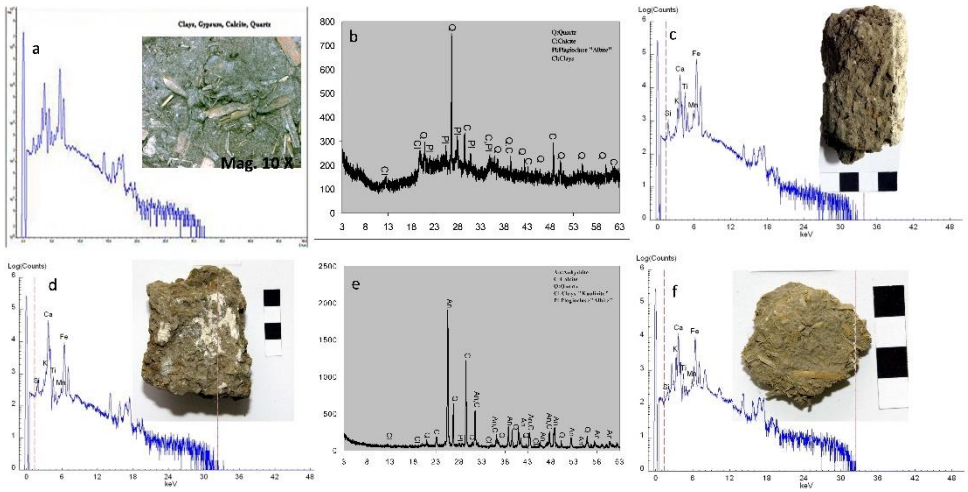

Figure 6. a & c) Macro-stereoscopic photograph 10 x magnification illustrates surface structure of clay mortar of tomb of Daji, Al-Qurna showing shaped straw and clay mortar respectively with μ-XRF patterns; b) XRD pattern of clay mortar, d & f) Stereoscopic photographs of two hiba mortars from tombs Amen Em Ha and Kha' Em Het respectively accompanied with μ-XRF patterns, e) XRD pattern of hiba mortar.

In the context of petrographic analysis conducted on the limestone utilized in the region, as well as the clay plaster applied to Theban tomb TT-111 as an illustrative case, microphotographs (Figure 7) reveal insights into the texture and mineralogical composition. Specifically, the limestone sample predominantly comprises calcium carbonate mud, interspersed with microfossils exhibiting subtle iron-bearing mineral coatings. This rock exhibits notable porous structure and might be falls under the classification of fossiliferous micrite/mudstone. It is microcrystalline, with fine-grained crystals containg minor impurities, (clay minerals, quartz, and iron oxides).

As for the clay mortar, it incorporates chopped straw as fibrous additives, embedded within the clay matrix and surrounded by small quartz grains. These grains exhibit a combination of rounded and platy shapes, with some irregularities. Additionally, a few opaque minerals, potentially iron oxides, appear as black grains. The specimen will undergo independent processing along with other samples for the study of clay mineralogy, as detailed in Section 3.5. Image analysis using Jmicrovision on a stitched panorama microphotograph of pigmented clay plaster from tomb TT111, attributed to Amenwahsu, indicates a component ratio of approximately 34.2% aggregate, divided into 27.2% very fine sands (up to 0.3 mm) and 7% organic matter, primarily represented by straw with a maximum length of 2 mm,while clay particles exhibits 65.8%.

 doi:10.20944/preprints202405.0634.v1

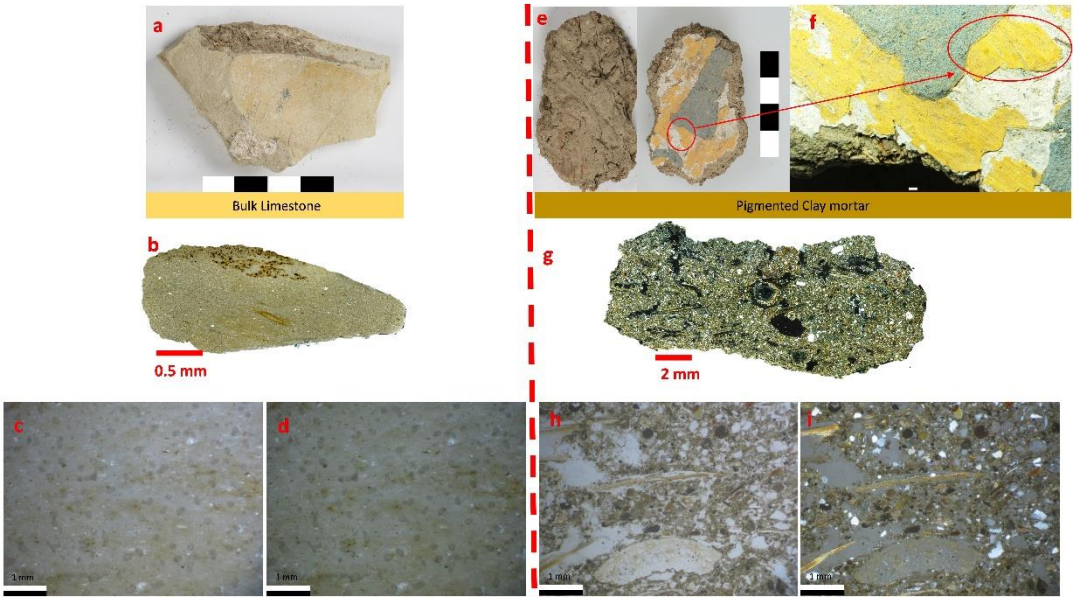

Figure 7. a) Bulk limestone from TT111, b) Stitched panoramic microphotograph in cross polarized light, c,d) Microphotographs of TT-111 limestone under both plane-polarized and cross-polarized light respectively, e, f) stereomicro/ magnified macroscopic photographs of pigmented clay mortar from TT-111, g) Stitched panoramic microphotograph in cross polarized light, h, i) Microphotographs of TT-111 clay mortar under both plane polarized and cross-polarized light respectively.

3.4. Microstructure by SEM and Chemical Elemental Analysis by EDS

Obtained results through scanning electron microscopy to analyze the microstructural characteristics of all components, in conjunction with elemental analysis by energy-dispersive X-ray spectroscopy (EDS), are presented in Figure 8 and Tables 3 and 4. The tabulation of mineral oxides present in the Esna shale indicates a significant concentration of ferrous oxides in the specimen, which suggests the provenance of the sediments in the region.

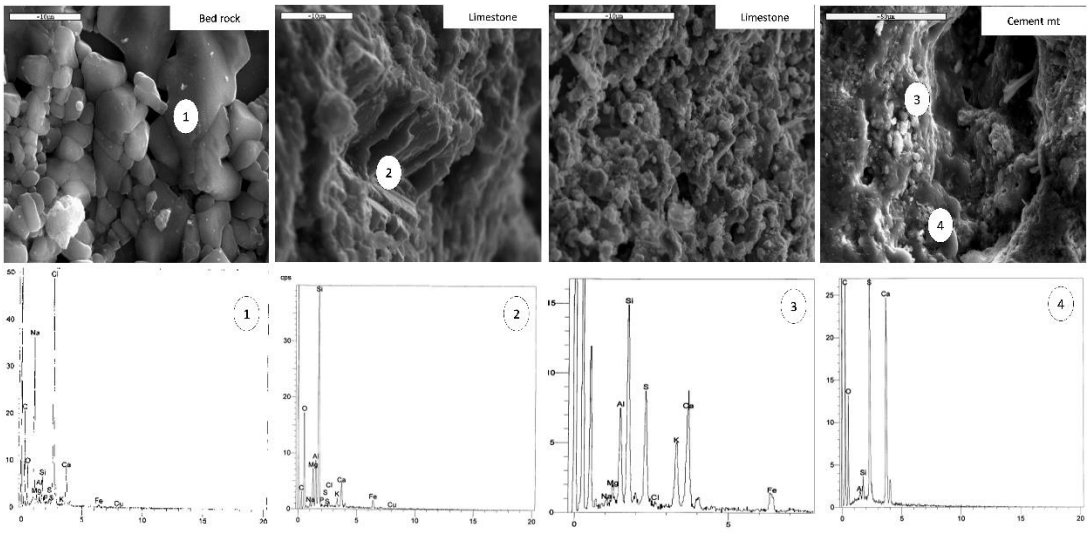

Figure 8. 1) SEM microphotograph illustrating the deposition of halite, pyrite, and quartz crystals within the Esna Shale with EDS spectra indicating the presence of Na.Cl, SiO_2, FeS and CaO. , 2) A pair of SEM microphotographs depicting the formation of clay nodules amidst the calcite crystals in the limestone specimen, with SEM-EDS spectra demonstrating the metamorphic transition from soft limestone to marl, 3 & 4) SEM microphotograph reveals the chemical composition of the cement material highlighting the presence of halite crystals within the cement matrix.

 doi:10.20944/preprints202405.0634.v1

Table 3. The chemical composition of the siliceous limestone and cement substance situated between the strata of limestone in Al-Qurna.

Siliceous limestone	Element %	Na	Mg	Al	Si	K	Ca	Fe	O	P	S	Mn	Ni	Total
		5.52	0.43	3.11	11.82	0.58	42.29	0.63	35.62	-	-	-	-	100%
	Atomic %	5.86	0.43	2.81	10.26	0.36	25.73	0.27	54.28	-	-	-	-	100%
	Compound %	Na2O	MgO	Al2O3	SiO2	K2O	CaO	FeO	-	-	-	-	-	-
		7.45	0.71	5.89	25.29	0.7	59.17	0.81	-	-	-	-	-	100%
Cement material between the limestone layers	Element%	Na	Mg	Al	Si	K	Ca	Fe	O	P	S	Mn	Ni	Total
		0.24	0.34	0.04	0.16	0	69.87	0.51	28.85	0.09	0.16	0.28	0.51	100%
	Atomic %	0.24	0.39	0.04	0.16	0	48.56	0.25	50.23	0.08	0.14	0.14	0.24	100%
	Compound %	Na2O	MgO	Al2O3	SiO2	K2O	CaO	FeO	-	P2O5	SO3	MnO	NiO	-
		0.27	0.56	0.07	0.34	0	97.76	0.65	-	0.21	0.41	0.37	0.64	100%

Table 4. Quantitative mineralogical constituents (by weight percentage) of studied specimens from Al-Qurna.

Samples	An	C	Q	Pl	Ha	M	Do	Cl
Esna shale	-	24	10	-	6	-	22	
Hard limestone	-	100	-	-	-	-	-	-
Soft limestone	29	27	-	-	-	-	44	-
Cement material	-	96	2	-	2	-	-	-
Clay mortar	-	24	50	10	-	-	-	16

An (Anhydrite), **C** (Calcite), **Q** (Quartz), **Pl** (Plagioclase), **Ha** (Halite), **M** (Micas), **Do** (Dolomite), and **Cl** (Clay minerals).

3.5. Clay Mineralogy

The results of clay mineralogical composition of the entire structure, including the bedrock (Esna shale), limestone, cementitious substances, and mortars, was characterized through X-ray diffraction (XRD) analysis employing three distinct sample preparations oriented, glycolated, and thermally treated are shown in Figure 9. This analytical approach was undertaken to evaluate the effect of these minerals on the progressive degradation of the wall paintings within the Qurna structures. Two samples of Esna shale (one dark grey and the other light grey) were procured from Al-Qurna. The initial one, a dark grey shale, was obtained from a burial well adjacent to Rekhmire tomb revealed during the oriented phase analysis, a mixed layer of illite-vermiculite (comprising 65%) at 7.20 - 7.30 Å. Additionally, an illite layer (constituting 35%) was observed at 8.38 Å. Subsequent glycolation revealed a new smectite layer (55.33%) at 5 - 5.14 Å, while the illite-vermiculite mixed layer persisted at 7.30 Å with a reduced volume (23.84%). Another illite sheet was also observed at the typical angle (8.38 Å). Upon heating, the clay minerals—smectite, illite-vermiculite mixed sheet, and illite—converged into a single curve spanning from 7.3 Å to 9.6 Å [Figure 9a]. The second sample, characterized by its light grey color, originates from the surficial Esna shale deposits within the study area. During the oriented phase analysis, this sample exhibits a mixed layer of illite-smectite spanning 6.5 Å to 7.5 Å. Subsequent glycolation results in the disappearance of the illite-smectite mixed sheet, with no discernible evidence of other clay minerals in the XRD pattern. Upon heating at 550°C for two hours, the illite-smectite mixed sheets reappears, albeit at a different range (8.6 Å to 9.2 Å), [Figure 9b]. The soft limestone sample that represents formations from which the majority of the tombs in Al-Qurna revealed constitute during the oriented phase analysis [Figure 9c], the presence of a smectite sheet at 5.13 Å and a halloysite at 11.55 Å. Following glycolated stage, these typical clay sheets persisted at the identical angles. However, upon heating, both clay layers dissipated. As for the cement substance situated amid the limestone strata within the studied area, during the oriented phase, an illite clay layer was discerned within the range of 3.25 – 8.27 Å. Subsequent glycolated treatment revealed the persistence of the same illite layer, now spanning 5.13 – 8.23 Å. Upon heating, the illite sheet shifted to 3.29 – 8.61 Å [Figure 9d]. Regarding the honeycomb weathering sample analyzed previously, it exhibited two distinct clay layers at 7.04 Å and 8.34 Å . However, these clay

Preprints.org (www.preprints.org) | NOT PEER-REVIEWED | Posted: 10 May 2024 doi:10.20944/preprints202405.0634.v1

layers remained unidentified until subjected to glycolation and heating treatments. After glycolation, the two clay sheets separated into three distinct ones: an illite-smectite mixed sheet at 4.98 Å, an illite-vermiculite mixed sheets at 7.14 Å, and a pure illite sheet at 8.23 Å . Upon heating, these three layers converged into a single peak at 8.94 Å, encompassing the illite-smectite mixed layer, illite-vermiculite mixed layer, and pure illite [Figure 9e]. Additionally, the Hiba mortar, derived from Amenemhab tomb, underwent geochemical separation to identify its clay mineral content. In the oriented phase, the sample revealed an unidentified clay sheet at 7.26 Å, along with a chlorite layer at 11.58 Å and a kaolinite layer at 12.28 Å. Following glycolation, the sample exhibited a swelling clay layer spanning 3.14 Å to 5.35 Å, in addition to the chlorite and kaolinite layers. Upon heating, these three layers coalesced into a continuous curve ranging from 3.32 Å to 8.76 Å [Figure 9f]. A clay mortar extracted from Daji tomb revealed during the oriented phase, distinct layers were identified: a swelling clay layer at 8.72 Å and a kaolinite layer at 12.24 Å. Subsequent glycolation revealed the persistence of these same layers, albeit at different positions: an expandable clay layer at 5.23 Å and a kaolinite layer at 12.27 Å. Upon heating, both clay layers coalesced into a single swelling clay layer, spanning from 3.13 Å to 8.84 Å [Figure 9g]. Another clay mortar sample [Figure 9h], sourced from Amen Em Hab tomb, exhibited distinct mineralogical features. In the oriented phase, the sample contained an unidentified clay layer at 6.73 Å, an illite layer at 8.77 Å, another unidentified clay layer at 9.78 Å, an amphibole layer at 10.4 Å, and a kaolinite layer at 12.3 Å. Following glycolation, a swelling clay layer emerged at 4.8 Å, accompanied by an illite sheet at 8.73 Å. Interestingly, the amphibole layer reappeared at the same angle (10.36 Å), as did the kaolinite sheet (12.23 Å). Upon heating, the two swelling clay layers, possibly containing smectite, merged into a single layer alongside illite (ranging from 3.05 Å to 8.77 Å), while the amphibole layer resurfaced at 10.44 Å.

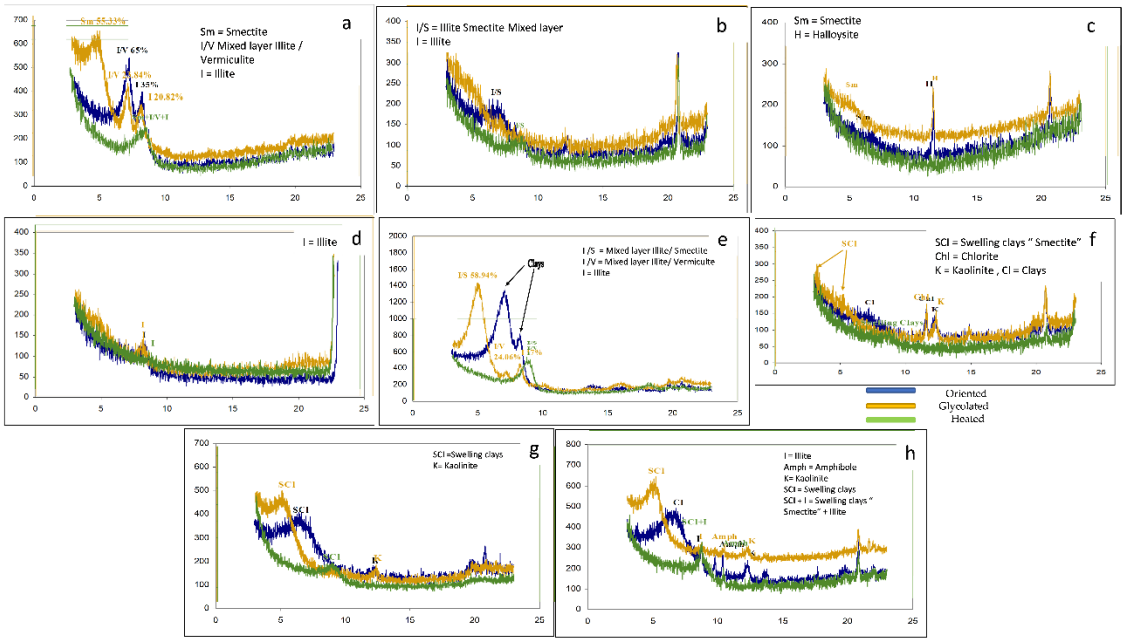

Figure 9. XRD patterens employing three distinct sample preparations oriented, glycolated, and thermally treated of a) An exemplar of Esna shale, characterized by its dark grey hue, sourced from the Al-Qurna Esna Shale formation, b) light grey Esna shale sample, c) soft limestone sample, d) cement material sample from Al-Qurna, e) honey comb weathering sample, f) hiba mortar sample, g) clay mortar from Daji tomb, h) clay mortar from Amen Em Hab tomb.

4. Discussion

The results from diverse examinations as a tool for monitoring in macro and micro scale of the current state of the studied area, particularly the initial visual assessment, on-site inspection of the wall paintings in Al-Qurna reveal that the causes of damage -in addition to human factors- can be categorized into two distinct categories: a) Direct Impact on inner surface and b) internal factors of

 doi:10.20944/preprints202405.0634.v1

the whole structure and surrounding soil. The former exclusively affects the inner surface and go deeper. This surface contains the pigmented layer within the various tombs. As a consequence, it -in turn- is divided into two parts, discoloration manifests as a physical consequence of staining caused by some isolated and identified fungal growth. Additionally, potential damage may arise from chemical reactions between metabolites and the constituents of the wall paintings, including pigments, media and substrate [39]. The latter incorporates the influence of internal factors arising from the composition of building materials and geological substrates. Notably, materials such as Esna Shale, limestone, and clay mortar contain harmful minerals that exert both mechanical and chemical effects on the wall paintings.

As for the microbiological identified species that represent the first category with both physical and chemical harmful effects can be extrapolated from species such as fungi *Ascosphaera apis* and *Aspergillus tamarii*; a species of fungus that belongs to the *Ascomycota phylum*. They are constituting 25% and 20 % respectively of the total fungal isolates. The former which has been identified on blue, green, and black pigments inside Rekhmire tomb as well as sandstone columns at Madinet Habu temple might cause biodegradative actions, including calcite dissolution, probability of binder hydrolysis, pigment secretion, and generation of alkalis and acids [40]. Consequently, the "acids" has an adverse effect where detrimental consequences of acid interactions encompass the disintegration of cations and the sequestration of metallic ions from both mortar and mineral pigments, which in turn instigates the creation of enduring metal complexes. The latter in case of crystallization within the painted stratum and mortar induces an escalation in internal pressure, which in turn increase subsequently provoking cracking and peeling, resulting in the eventual disintegration of mural segments [41,42]. This process of fungal invasion typically initiates at the surface level, subsequently penetrating deeper. This progression can lead to a reduction in the cohesion of the painted layer, instigating exfoliations and ultimately resulting in the loss of paint and detachment [43–45]. As for *Aspergillus occhraceus* representing 15% of the total isolated species, has indirect effect on the wall paintings, contributing to overall biodeterioration [46], which requires regular monitoring, preventive measures and special conservation actions to reduce its potential impact [47]. Additionally, it may lead to discoloration via staining and detachment [48]. *Doratomyces spp*, and *Eurotium chevalieri* [49] are also a genus of fungi that belongs to the *Ascomycota phylum*, but still need further research to determine exactly the mechanism of its impact on wall paintings especially on those bearing blue, black, white and green pigments. Finally, identified *Eurotium repens* -that has the ability to grow in environments with low a_w values and classified as extremophile organisms that can thrive under low-moisture conditions [50], can affect the organic binders causes reduction or even loss of paint layers [51], as well as penetrating cracks and migrating underneath paint layers resulting in detachment. The effect of *E. repens* in the overall ecosystem and potential impact should be well monitored and taken carefully into consideration especially in the tombs with high visitors' rates [52].

On the other hand, the identification of mineral oxides in the Esna shale by μ-XRF reveals a substantial concentration of iron oxides in the sample, which suggests the provenance of the sediments in the region. This presence is further corroborated by a petrographic analysis of the porous structure of limestone and clay mortar. This can be ascribed to the red clays and silt transported to Egypt by the Nile from the igneous mountains of Ethiopia; these alluvial deposits have influenced the chemical and physical geological structure along the Nile valley. This process has been halted since the construction of the high dam, which elevated the groundwater table of the country. SiO2 is a consequence of the Aeolian weathering of the aforementioned rocks, while MnO is likely responsible for the dark color of the Esna Shale, in conjunction with FeS, which was detected via SEM-EDS analysis [Figure 8]. CaO originates from the initial metamorphic limestone. For clay mortars, the appearance of iron oxides is due to a mixture rich in ferrous substances [53,54].

In Al-Qurna, the limestone stratum, under which the tombs were carved, is a hard white durable limestone that is badly jointed; this jointed nature impacts the upper applied wall paintings, resulting in the roof-cracking phenomenon [Figures 5b and 3L]. The XRD analyses of the hard limestone in the area confirmed that it is pure calcite 100%. Meanwhile, another limestone sample was taken from the rock formations in the area (the soft limestone stratum), this sample exhibits the so-called honeycomb

 doi:10.20944/preprints202405.0634.v1

weathering phenomenon, which occurs due to acid rain dissolving the salts and leaving holes on the limestone surface resembling a honeycomb. XRD analyses revealed that the sample is limestone transformed into gypsum by acid rain and then into anhydrite due to the effect of high temperature [55]; this transformation typically occurs on the stone surface, but the internal composition of the stone remains calcite and dolomite. The soft one consists of dolomite 44%, anhydrite 29%, and calcite 27% as shown in Table 4. This intricate interplay of mineral transformations offers valuable insights into the geological processes shaping the rock formations in the studied area. Using the μ-XRF analysis, the same results have been confirmed [Figure 5j]; no sulfur could be detected in the chart; sulfur, which was detected by the SEM, can also be a result of the air pollution in the area or a result of the biological growth on the stone surface. The precipitation of cement material veins between the limestone strata and inside the limestone fractures is one of the symptoms of the weathering process in the area [Figure 5d]; this cement material is usually weaker and more desiccated than the original stone, it may also contain a high quantity of soluble salts which may dissolve and migrate, leaving their places. The migration of the salts in with the vertical loads of the bed rocks may result in tectonic movements destroying the inside hewn tombs. The cement material was analyzed by means of SEM-EDS, which confirmed that it is of calcite mixed with traces of quartz, veins of silicon dioxide (SiO_2) and calcium chloride ($CaCl_2$) were also detected during the analysis process [Figure 8]; the latter is particularly dangerous especially when it dissolves and migrates, leaving pores in the stone structure, destroying the chemical bonds between calcite crystals, leading to the stone bleeding phenomenon, and the discoloring of the used pigment materials due to its efflorescence [56,57]. The high amount of sulfur may suggest the presence of pyrite in the sample; as shown in Table 3, it is assured that the main component of the sample is calcite while other compounds are just traces.

Regarding clay mortars, chloride salts sauch as NaCl and $CaCl_2$ and $CaSo_4$ were detected in a relatively high amount, which was also found in the limestone and cement material between limestone strata as well. That could indicate migration of various deliquesent types of salts from the starting point at Esna shale throught limestone of the tombs towards the supporting layers of wall paintings increasing propability of cracking and affecting pigments [58]. This problem is less effective in clay-based plaster layers containing fibrous binding materials, which enhance its mechanical properties [59]. In addition, to those salts, the presence of swelling clay minrals in whole structure incldуing Esna shale (both dark and light ones), limestone and even clay mortars where the wall painings have been applied, play a serious threatening role in damage process. Those clay minerals include smectite – which has remarkable ability to expand and contract significantly with changes in moisture [60]. This property can lead to cracking and flaking of the wall paintings via applying a considerable pressure on the structure of Esna shale, limestone and clay mortars bearing wall paintings affecting the stability of the Theban tombs. Illite-smectite mixed layers may show intermediate swelling behavior and Vermiculite has also a medium shrink–swell capacity, but it can still cause some degree of cracking and flaking of the wall paintings while halloysite has a low shrink-swell capacity [61,62]. However, the fine particle size and high plasticity of halloysite can affect the texture and appearance of the wall paintings. Illite clays are somewhere between [63]. In light of the aforementioned information, it is evident that deleterious clay minerals, characterized by their swelling properties, exist in varying proportions within each constituent of the construction materials and the adjacent geological formations. The availability of requisite moisture can potentially amplify the risk, posing a significant threat to the structural integrity of the tombs and the preservation of the invaluable artifacts they house. This underscores the critical need for comprehensive mineralogical assessments in such contexts as a tool of monitoring on the mineralogical scale beside other efforts of geological studies classifiyng lithologic units of Esna shale [64,65] and long-term monitoring of geological factors controlling the evolution of Theban tombs stability [66,67] preferably the none destructive techniques [68] as much as possible. In conclusion, the integrity of the wall paintings in Al-Qurna is intricately connected to its geological context, which includes the coexistence of the robust Thebes Limestone Formation and the relatively delicate Esna Shale Formation that underlies it. Mass movement phenomena, such as landslides or other forms of displacement, could potentially compromise stability due to the presence of the weaker shale as well as presnce of harmful clay

 doi:10.20944/preprints202405.0634.v1

minerals. Furthermore, an overabundance of iron content can induce color instability and adversely affect the durability of the plaster [69], thereby posing additional challenges to preservation efforts. For that, this work assurs that ongoing monitoring and maintainance are serious and highly required steps as indispensable strategies for preservation of those valuable wall paintings.

5. Conclusions

The wall paintings in Al -Qurna is subject to a multitude of hazards and diverse damage factors. This study highlights the detrimental impact of expanded clay minerals and microorganisms. The influence of each, either individually or together, contributes to the alteration of the structural integrity of the wall paintings and the construction materials derived from them. This results in a lack of stability in the tombs, accompanied by visible signs of damage such as delamination, flaking, color loss, and chromatic distortion. This highlights the need for comprehensive conservation strategies to mitigate these effects and preserve these invaluable cultural paintings. This study advocates for the sustained cyclical surveillance of the wall paintings structures and efforts towards the stabilization of the surrounding geological formations to mitigate the primary sources of damage. It further proposes routine upkeep of the pigmented surfaces, encompassing both chemical and mechanical cleaning methods, while considering the potential existence of hazardous microorganisms. Additionally, it is advisable to implement a range of preventative strategies to curtail the proliferation of diverse microorganisms, which includes regulating visitor traffic in areas accessible to the public. These recommendations underscore the importance of a holistic approach to the preservation of these invaluable cultural wall paintings.

Author Contributions: Conceptualization, A.M. and A.O.; Data curation, A.M. and A.O.; Investigation, A.M. and A.O.; Methodology, A.M. and A.O.; Writing–original draft, A.M. and A.O.; Writing–review & editing, A.M. and A.O.; All authors have read and agreed to the published version of the manuscript.

Funding: This research received no external funding.

Institutional Review Board Statement: Not applicable.

Informed Consent Statement: Not applicable.

Data Availability Statement: Data available upon request from the authors.

Acknowledgments: We would like to thank Dr. Nicolas Kantiranis from Aristotle University of Thessaloniki, Greece.

Conflicts of Interest: The authors declare no conflict of interest.

References

1. Said, R. (Ed.). The geology of Egypt. Routledge 2017. https://doi.org/10.1201/9780203736678
2. Reeves, N., Wilkinson, R.H. *The Complete Valley of the Kings: Tombs and Treasures of Egypt's Greatest Pharaohs*, American University of Cairo Press, Egypt, 1996.
3. Masanori, H., Aydan, O., Tano, H. A Report on Environmental and Rock Mechanical Investigations for the Conservation Project in the Royal Tomb of Amenophis III, Conservation of the Wall Paintings in the Royal Tomb of Amenophis III, First and Second Phases Report, (Yoshimura, S., Kondo, J., Ed.), under the Auspices of UNESCO / Japan Trust, Fund Joint Project of Supreme Council of Antiquities, Ministry of Culture, Arab Republic of Egypt and Institute of Egyptology, Waseda University, Japan, Akht Press, Printed in Tokyo, JAPAN, 2004.
4. Reeves, N., *News from the Valley of the Kings Foundation, Another new Tomb in the Valley of the Kings: 'KV64' - II*, Amarna Royal Tombs Project, Egypt-United Kingdom, 2006.
5. Weeks, K., Hetherington, N., *The Valley of the Kings Site Management Master plan,* The Theban Mapping Project "Egypt" in Co-Operation with Amazon, U.S.A, 2005.
6. Weeks, K., *The Illustrated Guide to Luxor Tombs, Temples and Museums,* The Theban Mapping Project "Egypt" in co-operation with Amazon, U.S.A, 2006.
7. King, C., Dupuis, C., Aubry, M., Berggren, W., Knox, R., Galal, W., Baele, J. Anatomy of a mountain: The Thebes Limestone Formation (Lower Eocene) at Gebel Gurnah, Luxor, Nile Valley, Upper Egypt, *Journal of African Earth Sciences* **2017**, *Volume 136*, pp. 61–108. https://doi.org/10.1016/j.jafrearsci.2017.05.008

8. Abd EL Hafez, N., Abd El-Moghny, M., El-hariri, T., Mousa, A., Hamed, T. Mineralogy and Depositional Environment of the Thebes Formation at the Area Between Safaga and Qusier Along Red Sea Coast, Egypt, Al Azhar Bulletin of Science **2017**, *Volume 28 (2)*, pp. 1–16.
9. El Ayyat, A., Obaidalla, N., Salman A., Sayed, M. Facies Analysis and Paleoenvironmental Reconstruction of the Thebes Formation (Lower Eocene) Sequence Along the Red Sea Coast Between Qusier and Hurghada, Egypt, *Assiut Univ. J. of Geology* **2021**, *Volume 50 (1)*, pp. 1–28. https://doi.org/10.21608/aunj.2021.219957
10. Taha, S., Late Paleocene–Early Eocene Foraminiferal Paleobathymetry and Depositional Environments and Their Sequence Stratigraphic Implications of Gebel Duwi, Red Sea, Egypt, *Egyptian Journal of Geology* **2023**, *Volume 67*, pp. 1–31. https://doi.org/10.21608/egjg.2023.188298.1034
11. McLane, J.; Wüst, R. Flood Hazards and Protection Measures in the Valley of the Kings, *CRM* **2000**, *Volume 6*, pp. 35–38.
12. Ortolani, F.; Pagliuca, S. Geoenvironmental Variations over the Last Millennia within the Mediterranean Area and Expected Influence of the next "Greenhouse Effect", In Proceedings of the International conference on Global Climate Changes During the Late Quaternary, Rome, Italy, 3–4 May 2001.
13. Anthony, F. B. *Foreigners in ancient Egypt: Theban tomb paintings from the early Eighteenth Dynasty*, Bloomsbury Publishing, 2016. https://doi.org/10.5040/9781474241618
14. Wilkinson, R. H., & Weeks, K. R. (Eds.). *The Oxford handbook of the Valley of the Kings*. Oxford University Press, 2016. https://doi.org/10.1093/oxfordhb/9780199931637.001.0001
15. Manniche, L. *The wall decoration of three Theban tombs (TT 77, 175, and 249)* (No. 4). Museum Tusculanum Press, 1988.
16. Laboury, D. Tracking Ancient Egyptian Artists, a Problem of Methodology. The Case of the Painters of Private Tombs in the Theban Necropolis During the Eighteenth Dynasty. *Art and Society Ancient and Modern Contexts of Egyptian Art*, Museum of Fine Arts, Budapest, Hungary, 2012.
17. Bryan, B. M. Painting Techniques and Artisan Organization in the Tomb of Suemniwet, Theban Tomb 92, *Colour and painting in ancient Egypt* **2001**, pp. 63–72.
18. Dodson, A., and Ikram, S. *The tomb in ancient Egypt: Royal and private sepulchres from the Early Dynastic Period to the Romans*, Thames and Hudson, 2008.
19. Weeks, K. R., Manferto, V., Accomazzo, L. (Eds.). *Valley of the Kings: The Tombs and the Funerary Temples of Thebes West*, White Star, 2011.
20. Riemer, W. Degrading Igneous Rock-Aspects and Identification of the Geotechnical Problem, Proceedings of the International Symposium on Industrial Minerals and Building Stones, Istanbul, 2003, pp. 841–848.
21. Kondratyeva, I.A., Gorbushina, A.A., Boikova, A.I. Biodeterioration of Construction Materials, *Glass Physics and Chemistry*, **2006**, *Volume 32 (2)*, pp. 254–256. https://doi.org/10.1134/s1087659606020209
22. Booth, C., *Methods in Microbiology*, 4th ed.; Academic Press, New York, 1971.
23. Stevens, R.B., *Mycology Guide Book*, Mycology Guide Book Committee, Mycology Society of American Universities, Washington Press, Seattle, U.S.A., 1981.
24. Barnett, H.L., Hunter, B.B., *Illustrated Genera of Imperfect Fungi*, 3rd ed.; Burgess Publication Con. Minneapolis, Minnesota, 1972.
25. Domsch, K.H. Gams, W., Anderson, T.H., *Compendium of Soil Fungi*, Volume 1 and 2, Academic Press, London, 1980.
26. Hemraj, H., Diksha, S., Avneet, G. A Review on Commonly Used Biochemical Test for Bacteria, *Innovare Journal of Life Science* **2013**, *Volume 1 (1)*, pp. 1–7.
27. Bergey. *Bergey's Manual of Systematic Bacteriology*, 2nd Ed., Volume 2, Part C, 2008.
28. Middendorf, B., Hughes, J. J., Callebaut, K., Baronio, G., Papayianni, I. Investigative Methods for the Characterization of Historic Mortars—part 1: Mineralogical Characterization, *Materials and Structures* **2005**, *Volume 38 (8)*, pp. 761–769. https://doi.org/10.1617/14281
29. Osman, A., Bartz, W., & Kosciuk, J. **2016**. Characterization of historical mortar used in loom factory site at Abydos. *Egyptian Journal of Archaeological and Restoration Studies*, *6(2)*, pp. 97-107. DOI: 10.21608/EJARS.2019.23629
30. Bartz, W., & Martusewicz, J. Terrazzo Floor from the Jewish Historical Institute in Warsaw–Mineralogical Characterization, Conservation and Impact of Fire, *Geoscience Records* **2017**, *Volume 4 (1)*, pp. 1–13. https://doi.org/10.1515/georec-2017-0001
31. De Luca, R., Ontiveros, M. C., Miriello, D., Pecci, A., Le Pera, E., Bloise, A., Crisci, G. M. Archaeometric Study of Mortars and Plasters from the Roman City of Pollentia (Mallorca-Balearic Islands), *Periodico di Mineralogia* **2013**, *Volume 82(3)*, pp. 353–379. https://doi.org/10.2451/2013PM0021
32. Miriello, D., Bloise, A., Crisci, G. M., De Luca, R., De Nigris, B., Martellone, A., Ruggieri, N. New Compositional Data on Ancient Mortars and Plasters from Pompeii (Campania–Southern Italy): Archaeometric Results and Considerations about their Time Evolution, *Materials Characterization* **2018**, *Volume 146*, pp. 189–203. https://doi.org/10.1016/j.matchar.2018.09.046

33. Blott, S. J., and Pye, K. GRADISTAT: A Grain Size Distribution and Statistics Package for the Analysis of Unconsolidated Sediments, *Earth surface processes and Landforms* **2001**, *Volume 26 (11)*, pp. 1237–1248. https://doi.org/10.1002/esp.261
34. JCPDS. *Jaint Committee on Powder Diffraction Standards*, Index to the Powder Diffraction File, American Society for Testing and Materials, Pennsylvania, 1967.
35. Folk, R.L. *Petrology of Sedimentary Rocks*, Hemphill's, Austin, Texas, 1968.
36. Jackson, M. L. *Soil Chemical Analysis*, Adv. Course. Madison, Winsconsin, 1974.
37. Pehlivanoglou, K., Tsirambides, A., Trontsios, G. Origin and Distribution of Clay Minerals in the Alexandroupolis Gulf, Aegean Sea, Greece, Estuarine, *Coastal and Shelf Science* **2000**, *Volume 51*, pp. 61–73. https://doi.org/10.1006/ecss.1999.0620
38. Biscaye, P. E., Mineralogy and Sedimentation of Recent Deep Sea Clay in the Atlantic Ocean and Adjacent Seas and Oceans, *Geological Society American Bulletin* **1965**, *Volume 76*, pp. 803–831. https://doi.org/10.1130/0016-7606(1965)76[803:MASORD]2.0.CO;2
39. Suphaphimol, N., Suwannarach, N., Purahong, W., Jaikang, C., Pengpat, K., Semakul, N., Disayathanoowat, T. Identification of Microorganisms Dwelling on the 19th Century Lanna Mural Paintings from Northern Thailand Using Culture-Dependent and-Independent Approaches, *Biology* **2022**, *Volume 11 (2)*, pp. 7–12. https://doi.org/10.3390/biology11020228
40. Unković, N., Dimkić, I., Stupar, M., Stanković, S., Vukojević, J., & Ljaljević Grbić, M. Biodegradative Potential of Fungal Isolates from Sacral Ambient: In Vitro Study as Risk Assessment Implication for the Conservation of Wall Paintings, *PLoS One* **2018**, *Volume 13 (1)*, DOI. 10.1371/journal.pone.0190922.
41. Moussa, A., Badawy, M., Saber, N. Chromatic alteration of Egyptian Blue and Egyptian Green Pigments in Pharaonic Late Period Tempera Murals, *Scientific Culture* **2021**, *Volume 7 (2)*, pp. 1–15. DOI: 10.5281/zenodo.4465458
42. Piñar, G., Ripka, K., Weber, J., Sterflinger, K. The Micro-Biota of a Sub-Surface Monument the Medieval Chapel of St. Virgil (Vienna, Austria). *International Biodeterioration & Biodegradation* **2009**, *Volume 63* (7), pp. 851–859. https://doi.org/10.1016/j.ibiod.2009.02.004
43. Ciferri, O. Microbial Degradation of Paintings, *Applied and Environmental Microbiology* **1999**, *Volume 65 (3)*, pp. 879–885. https://doi.org/10.1128/aem.65.3.879-885.1999
44. Rosado, T., Gil, M., Mirão, J., Candeias, A., & Caldeira, A. T. Oxalate Biofilm Formation in Mural Paintings Due to Microorganisms–A Comprehensive Study, *International Biodeterioration & Biodegradation* **2013**, *Volume 85*, pp. 1–7. https://doi.org/10.1016/j.ibiod.2013.06.013
45. Garg, K. L., Jain, K. K., & Mishra, A. K. Role of fungi in the deterioration of wall paintings, *Science of the Total Environment* **1995**, *Volume 167 (1-3)*, pp. 255–271. https://doi.org/10.1016/0048-9697(95)04587-q
46. Gorbushina, A. A., Heyrman, J., Dornieden, T., Gonzalez-Delvalle, M., Krumbein, W. E., Laiz, L., Swings, J. Bacterial and Fungal Diversity and Biodeterioration Problems in Mural Painting Environments of St. Martins Church (Greene–Kreiensen, Germany), *International Biodeterioration & Biodegradation* **2004**, *Volume 53 (1)*, pp. 13–24. https://doi.org/10.1016/j.ibiod.2003.07.003
47. Zucconi, L., Canini, F., Isola, D., & Caneva, G. Fungi Affecting Wall Paintings of Historical Value: A Worldwide Meta-Analysis of their Detected Diversity, *Applied Sciences* **2022**, *Volume 12 (6)*, 2988. https://doi.org/10.3390/app12062988
48. Pepe, O., Palomba, S., Sannino, L., Blaiotta, G., Ventorino, V., Moschetti, G., & Villani, F. Characterization in the Archaeological Excavation Site of Heterotrophic Bacteria and Fungi of Deteriorated Wall Painting of Herculaneum in Italy, *Journal of Environmental Biology* **2011**, *Volume 32 (2)*, pp. 241–250.
49. Eurotium chevalieri - Morphology, Health Effects and Treatment (bustmold.com)
50. Eurotium repens - Habitat, Reproduction and Health Effects (bustmold.com)
51. Sterflinger, K. Fungi: Their Role in Deterioration of Cultural Heritage, *Fungal Biol Rev* **2010**, *Volume 24*, pp. 47–55. https://doi.org/10.1016/j.fbr.2010.03.003
52. Viñals, M. J., & Lull, J. Tourism Potential of the Sheikh Abd El-Qurna Tombs (West Bank of Luxor, Egypt), *Methods and Analysis on Tourism and Environment* **2013**, pp. 19-29.
53. Moussa, A., Kantiranis, N., Voudouris, K., Stratis, J., Ali, M., Christaras, V. The Impact of Soluble Salts on the Deterioration of Pharaonic and Coptic Wall Paintings at Al Qurna, Egypt: Mineralogy and Chemistry, *Archaeometry* **2009**, *Volume 51 (2)*, pp. 292–308, doi: 10.1111/j.1475-4754.2008.00422.x
54. Singh, M., Kumar, S. V., Waghmare, S. Mud Plaster Wall Paintings of Bhaja Caves: Composition and Performance Characteristics, *Indian Journal of History of Science* **2016**, *Volume 51(3)*, pp. 431–442. https://doi.org/10.16943/ijhs/2016/v51i3/48846
55. Cuezva, S., García-Guinea, J., Fernandez-Cortes, A., Benavente, D., Ivars, J., Galan, J. M., Sanchez-Moral, S. Composition, Uses, Provenance and Stability of Rocks and Ancient Mortars in a Theban Tomb in Luxor (Egypt), *Materials and structures* **2016**, *Volume 49*, pp. 941–960. https://doi.org/10.1617/s11527-015-0550-5
56. Piqué, F., Dei, L., & Ferroni, E. Physicochemical Aspects of the Deliquescence of Calcium Nitrate and its Implications for Wall Painting Conservation, *Studies in conservation* **1992**, *Volume 37 (4)*, pp. 217–227. https://doi.org/10.2307/1506351

57. Zehnder, K. Long-Term Monitoring of Wall Paintings Affected by Soluble Salts, *Environmental Geology* **2007**, *Volume 52*, pp. 353–367. https://doi.org/10.1007/s00254-006-0463-2
58. Mohie, M.A. and Moussa, A. Diagnosis of Pigment Materials Affected by Air Pollution and Clay Minerals in Sabil Alkazlar, *Annales islamologiques* **2011**, *Volume 45*, pp. 321–338.
59. Singh, M., and Arbad, B. R. Scientific Studies on Decorated Mud Mortar of Ajanta, *Case Studies in Construction Materials* **2014**, *Volume 1*, pp. 138–143. https://doi.org/10.1016/j.cscm.2014.07.001
60. Derkowski, A., and Kuligiewicz, A. Thermal Analysis and Thermal Reactions of Smectites: A Review of Methodology, Mechanisms, and Kinetics, *Clays and Clay Minerals* **2022**, *Volume 70 (6)*, pp. 946–972. https://doi.org/10.1007/s42860-023-00222-y
61. Tamsu Selli, N., Aker, I. M., Basaran, N., Kabakci, E. L. İ. F. Influence of Calcined Halloysite on Technological & Mechanical Properties of Wall Tile Body, *Journal of Asian Ceramic Societies* **2021**, *Volume 9 (3)*, pp. 1331–1344. https://doi.org/10.1080/21870764.2021.1974762
62. Lampropoulou, P., & Papoulis, D. Halloysite in Different Ceramic Products: A Review, *Materials* **2021**, *Volume 14 (19)*, 5501. https://doi.org/10.3390/ma14195501
63. Millrath, K., Kozlova, S., Meyer, C., Shimanovich, S. *New Approach to Treating the Soft Clay / Silt Fraction of Dredged Material*, Echo Environmental, Inc., Columbia University, New York, 2002. https://doi.org/10.1061/40680(2003)138
64. Aubry, M. P., Berggren, W. A., Dupuis, C., Ghaly, H., Ward, D., King, C., Galal, W. F. Pharaonic Necrostratigraphy: A Review of Geological and Archaeological Studies in the Theban Necropolis, Luxor, West Bank, Egypt, *Terra Nova* **2009**, *Volume 21 (4)*, pp. 237–256. https://doi.org/10.1111/j.1365-3121.2009.00872.x
65. El-Shater, A., Mansour, A., Osman, M., Abd El Ghany, A., Abd El-Samee, A. Evolution and Significance of Clay Minerals in the Esna Shale Formation at Dababiya Area, Luxor, Egypt, *Egyptian Journal of Petroleum* **2021**, *Volume 30 (2)*, pp. 9–16. https://doi.org/10.1016/j.ejpe.2021.03.001
66. Wolter, A., Ziegler, M., Colldeweih, R., Loprieno-Gnirs, A., Alcaino-Olivares, R., Perras, M. Geological Factors Controlling Evolution of Theban Tomb Stability, Luxor, *Sustainable Conservation of UNESCO and Other Heritage Sites Through Proactive Geosciences* **2023**, pp. 429–442. https://doi.org/10.1007/978-3-031-13810-2_23
67. Gelany, A., Zeid, M., Abd El-Sadek, M., Mansour, A. Evaluation of the Expansive Esna Shale and its Role in the Deterioration of Heritage Buildings at West Bank of Luxor, *Journal of Geoscience and Environment Protection* **2019**, *Volume 7 (8)*,pp. 24–37. https://doi.org/10.4236/gep.2019.78002
68. Vandenabeele, P., Garcia-Moreno, R., Mathis, F., Leterme, K., Van Elslande, E., Hocquet, F. P., Hartwig, M. Multi-disciplinary Investigation of the Tomb of Menna (TT69), Theban Necropolis, Egypt, *Spectrochimica Acta Part A: Molecular and Biomolecular Spectroscopy* **2009**, *Volume 73 (3)*, pp. 546–552. https://doi.org/10.1016/j.saa.2008.07.028
69. Sharma, A., and Singh, M. A Review on Historical Earth Pigments Used in India's Wall Paintings, *Heritage* **2021**, *Volume 4 (3)*, pp. 1970–1994. https://doi.org/10.3390/heritage4030112